Genetic basis of neurocognitive decline and reduced white-matter integrity in normal human brain aging

David C. Glahn[a,b,1], Jack W. Kent, Jr.[c], Emma Sprooten[a,b], Vincent P. Diego[c], Anderson M. Winkler[a,b], Joanne E. Curran[c], D. Reese McKay[a,b], Emma E. Knowles[a,b], Melanie A Carless[c], Harald H. H. Göring[c], Thomas D. Dyer[c], Rene L. Olvera[d], Peter T. Fox[e], Laura Almasy[c], Jac Charlesworth[f], Peter Kochunov[g], Ravi Duggirala[c], and John Blangero[c]

[a]Olin Neuropsychiatry Research Center, Institute of Living, Hartford Hospital, CT 06106; [b]Department of Psychiatry, Yale University School of Medicine, New Haven, CT 06511; [c]Department of Genetics, Texas Biomedical Research Institute, San Antonio, TX 78227; [d]Department of Psychiatry, University of Texas Health Science Center at San Antonio, San Antonio, TX 78229; [e]Research Imaging Institute, University of Texas Health Science Center at San Antonio, San Antonio, TX 78229; [f]Menzies Research Institute Tasmania, University of Tasmania, Hobart, Tasmania 7000, Australia; and [g]Maryland Psychiatric Research Center, Department of Psychiatry, University of Maryland School of Medicine, Catonsville, MD 21228

Edited by Stephen T. Warren, Emory University School of Medicine, Atlanta, GA, and approved October 8, 2013 (received for review July 22, 2013)

Identification of genes associated with brain aging should markedly improve our understanding of the biological processes that govern normal age-related decline. However, challenges to identifying genes that facilitate successful brain aging are considerable, including a lack of established phenotypes and difficulties in modeling the effects of aging per se, rather than genes that influence the underlying trait. In a large cohort of randomly selected pedigrees (n = 1,129 subjects), we documented profound aging effects from young adulthood to old age (18–83 y) on neurocognitive ability and diffusion-based white-matter measures. Despite significant phenotypic correlation between white-matter integrity and tests of processing speed, working memory, declarative memory, and intelligence, no evidence for pleiotropy between these classes of phenotypes was observed. Applying an advanced quantitative gene-by-environment interaction analysis where age is treated as an environmental factor, we demonstrate a heritable basis for neurocognitive deterioration as a function of age. Furthermore, by decomposing gene-by-aging (G × A) interactions, we infer that different genes influence some neurocognitive traits as a function of age, whereas other neurocognitive traits are influenced by the same genes, but to differential levels, from young adulthood to old age. In contrast, increasing white-matter incoherence with age appears to be nongenetic. These results clearly demonstrate that traits sensitive to the genetic influences on brain aging can be identified, a critical first step in delineating the biological mechanisms of successful aging.

neurocognition | diffusion tensor imaging | fractional anisotropy | genetic correlation | gene x environment interaction

Population projections suggest for the first time in human history there will be more individuals over the age of 65 than below the age of 14 by 2050 (1). This milestone reflects the dramatic increase of the average lifespan of people worldwide, rather than a reduction in the total number of children being born. Indeed, 25% of the US population is expected to be over the age of 60 midway through this century (1). The implications of our aging population are substantial, because aging is associated with decreased mental and physical ability coupled with increased health care utilization. Thus, there is considerable interest in delineating the biological mechanisms that influence age-related changes to facilitate successful aging (2), defined as avoidance of disease or disability, maintaining good physical and cognitive function, and engagement in social and productive activities. Because the brain appears to play a pivotal role in aging biology (3), one promising strategy is to define measures of brain structure and function that index concomitant aging outcomes (4). The observation that many measures of brain aging are heritable and can be localized to specific genomic regions (6) indicates that genetic factors play a crucial role in the brain's ability to either prosper or deteriorate with age. The identification of successful brain aging genes should provide important insights into the biological mechanisms that foster prolonged vitality. Such insights should lead to enhanced prediction models and potential interventions that could improve the quality of life of older individuals. Unfortunately, the challenges to identifying brain aging genes are considerable and include a lack of established phenotypes (5) and difficulties in modeling the effects of aging that are at least partially independent of the underlying trait (e.g., identifying genes associated with immune function generally rather than those associated with the ability to ward off infection with age).

Neurocognitive measures are important indices of brain aging because processing speed, memory, and executive function tests are reliable, heritable, and dramatically influenced by normal and pathological aging (6, 7). Therefore, identifying genetic factors associated with age-related cognitive decline could have a profound impact on our understanding of the underlying biology that influences brain function over the lifespan (8). Similarly, in vivo measurements of white-matter integrity provided by diffusion tensor imaging (DTI) are fitting brain-aging phenotypes because these heritable traits are particularly sensitive to healthy and pathological aging (9, 10). Indeed, changes in fractional anisotropy (FA) as indexed by DTI appear to be among the most sensitive neuroimaging measures of the degeneration observed in normal and abnormal aging (11) and of

Significance

Identification of genes associated with brain aging should improve our understanding of the biological processes that govern normal age-related decline. In randomly selected pedigrees, we documented profound aging effects from young adulthood to old age (18–83 years) on neurocognitive ability and diffusion-based white-matter measures. Despite significant phenotypic correlation between white-matter integrity and tests of processing speed, working memory, declarative memory, and intelligence, no evidence for shared genetic determination was observed. Applying a gene-by-environment interaction analysis where age is an environmental factor, we demonstrate a heritable basis for neurocognitive deterioration with age. In contrast, increasing white-matter incoherence with age appears to be nongenetic. Identifying brain-aging traits is a critical first step in delineating the biological mechanisms of successful aging.

Author contributions: D.C.G., J.E.C., H.H.H.G., R.L.O., P.T.F., L.A., R.D., and J.B. designed research; D.C.G., R.L.O., P.T.F., P.K., R.D., and J.B. performed research; D.C.G., J.W.K., E.S., V.P.D., A.M.W., D.R.M., E.E.K., H.H.H.G., T.D.D., L.A., J.C., and J.B. analyzed data; and D.C.G., J.W.K., E.S., A.M.W., J.E.C., D.R.M., E.E.K., M.A.C., H.H.H.G., L.A., J.C., P.K., and J.B. wrote the paper.

The authors declare no conflict of interest.

This article is a PNAS Direct Submission.

[1]To whom correspondence should be addressed. E-mail: david.glahn@yale.edu.

This article contains supporting information online at www.pnas.org/lookup/suppl/doi:10.1073/pnas.1313735110/-/DCSupplemental.

age-related neurocognitive decline (12). However, reports associating white-matter integrity and cognitive aging are inconsistent, with some suggesting localized effects (13–17) and others pointing to global white-matter changes as the best predictors of age-related cognitive changes (18). Evidence for pleiotropy between neurocognitive and white-matter traits is sparse (19, 20), raising the possibility that age-related declines in these two classes of phenotypes may reflect independent genetic pathways. Regardless of whether they interact directly, neurocognitive performance and white-matter measurements are powerful classes of phenotypes for the discovery of brain aging genes.

Because the incremental increase in age over time is not the direct consequence of gene action, one can consider aging an effect of the environment. In this context, aging can be modeled as a gene-by-environment interaction (G × E). Generally, a significant G × E interaction is evidence for a heritable basis of a biological response to environmental change. A fundamental advantage of focusing on the G × E interaction for modeling the influence of genes on brain aging is that, given pedigree-based sampling, the interaction can be evaluated even when direct within-individual measurement of the trait's response to aging is not possible (21). Thus, a cross-sectional pedigree design that models the observed correlations between individuals as a function of both biological relatedness and environmental similarity enables testing of a gene-by-aging (G × A) interaction by examining heritable phenotypic change with advancing age between related individuals. In such a G × A analysis, the genetic variance (σ_g^2) of a given trait is allowed to vary with age, modeling potential differences in the scale of gene action over time. In addition, the genetic correlation between observations of a trait at different ages (ρ_g), expected to be 1 in the absence of age effects, may be a function of the difference in ages for any pair of observations of related individuals, suggesting that the relative effect sizes of the genes contributing to a trait vary with age. Thus, in addition to providing an estimate of genetic influences on aging, a G × A analysis suggests whether this genetic effect is likely due to fluctuations in the action of specific genes (changes in σ_g^2), variation in the exact genes influencing the trait at different ages (changes in ρ_g), or both. Kent and coworkers (22) recently used a similar analytic approach to identify over 600 lymphocyte-based RNA transcripts with significant G × A interactions, defining candidate genes for biological aging.

In the current report, we modeled advancing age, from young adulthood to old age, on cross-sectional measures of neurocognitive function and white-matter integrity in large randomly ascertained extended pedigrees. Our goals were to (*i*) document age-related changes in these indices of successful brain aging, (*ii*) further establish the heritability of these phenotypes, (*iii*) examine phenotypic, genetic, and environmental correlations between these classes of phenotypes, and (*iv*) determine if gene-by-aging interactions influence neurocognition and white-matter integrity.

Results

Age Distribution. Some 1,129 individuals from randomly selected extended pedigrees participated in the study. Age ranged from 18 to 83 y, with a mean of 44.17 (SD = 14.04; Fig. 1*A*). Average education was 11.99 ± 2.86 y (range 0–25). Sixty-two percent of the participants were female (n = 700). Ninety-eight percent of the sample (n = 1,112) had neurocognitive data, and 768 had high-quality DTI data (68%). In total, 751 individuals had both neurocognitive and DTI data that passed quality control assessments.

Aging and Neurocognition. Older subjects performed significantly worse than younger individuals on all neurocognitive measures (Table 1 and Fig. 1*B*). Measures of processing speed (e.g., Digit–Symbol Substitution and Trails A), working memory/executive functioning (e.g., Letter–Number Span and Matrix Reasoning), and declarative memory [California Verbal Learning Test (CVLT) Learning and Penn Facial Memory Delay] showed particularly substantial age-related declines. For example, average performance on a computerized Digit–Symbol Substitution task (23), a quintessential index of processing speed (24), decreased by 2.6 SDs from ages 18 to 83 (e.g., standardized β of −0.043, indicating a performance reduction of 0.04 SD units each year over the 65-y range of the sample).

Aging and White Matter. Tract-based FA measures uniformly decreased with advancing age (Table 1 and Figs. 1*C* and 2). Though the effects of aging differed somewhat between tracts, the overwhelming trend was a near-linear decrease in white-matter coherence with aging. For example, global FA, the average FA over the white-matter skeleton, decreased by 0.037 SD units per year from young adulthood to old age.

Phenotypic Correlation Between Neurocognition and White-Matter Integrity. Phenotypic correlations (ρ_p) between each neurocognitive and white-matter measure were performed while allowing for the effects of age and sex on individual-specific expected means. Consistent with the literature (16, 25–27) and after controlling for multiple testing, 33 significant correlations were observed (Fig. 3 and Table S1). For example, global FA was significantly correlated with Digit–Symbol Substitution (ρ_p = 0.11, P = 0.001), Trails A (ρ_p = −0.11, $P = 3 \times 10^{-4}$), Semantic Fluency (ρ_p = 0.11, P = 0.003), Letter–Number Span (ρ_p = 0.13, $P = 3 \times 10^{-4}$), Penn Facial Memory (ρ_p = 0.09, P = 0.001), and Matrix Reasoning (ρ_p = 0.13, P = 0.002). Similarly, Digit–Symbol Substitution was correlated with the splenium of the corpus callosum (ρ_p = 0.10, P = 0.001), the anterior (ρ_p = 0.10, P = 0.002), and posterior (ρ_p = 0.09, P = 0.003) limbs, and of internal capsule and the anterior (ρ_p = 0.12, $P = 1 \times 10^{-4}$) and posterior (ρ_p = 0.13, $P = 3 \times 10^{-4}$) corona radiate.

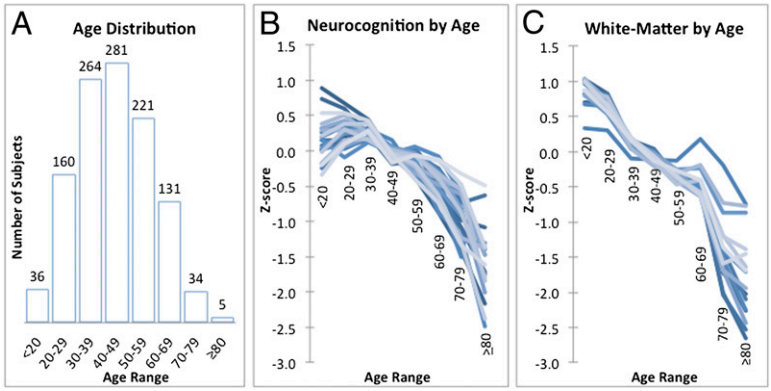

Fig. 1. The distribution of age (*A*) and its impact on neurocognitive function (*B*) and DTI-derived measures of white-matter integrity (*C*) in the Genetics of Brain Structure and Function Study cohort (n = 1,129). (*A*) Histogram representing the age distribution of study participants. Subjects' ages ranged from 18 to 83, with a mean of 45.82 ± 14.82. (*B*) Performance after z-transformation on each of the 22 neurocognitive variables stratified by the participant age. Though there is some test-specific variability, the overwhelming trend is for dramatic age-related declines across all neurocognitive measures. (*C*) Comparable to *B*, but reflects 17 tract-based measures of white-matter integrity changes with advancing age.

Table 1. Heritability estimates, effects of age and sex, and G × A interactions

Trait	Heritability h^2 (*P* value)	Age β (*P* value)	Sex β (*P* value)	σ_g^2 with age γ (*P* value)	ρ_g with age λ (*P* value)
Semantic Fluency	**0.37 (2×10^{-11})**	**−0.02 (1×10^{-16})**	−0.05 (0.419)	**−0.038 (0.003)**	0.006 (0.318)
Verbal Fluency	**0.50 (2×10^{-21})**	**−0.02 (2×10^{-12})**	0.04 (0.508)	−0.006 (0.591)	**0.022 (0.005)**
Digit–Symbol Substation	**0.52 (2×10^{-19})**	**−0.04 (2×10^{-107})**	0.10 (0.040)	**−0.037 (0.001)**	0.009 (0.142)
Trails A	**0.24 (2×10^{-6})**	**0.03 (7×10^{-45})**	**−0.27 (2×10^{-6})**	0.007 (0.607)	**0.060 (0.002)**
IP-CPT Hits	**0.28 (8×10^{-7})**	**−0.01 (0.016)**	−0.13 (0.038)	−0.015 (0.497)	0.030 (0.042)
IP-CPT FA	**0.32 (1×10^{-9})**	**0.02 (7×10^{-18})**	**0.22 (2×10^{-4})**	−0.021 (0.076)	0.028 (0.034)
Digit Span Forward	**0.39 (6×10^{-13})**	**−0.02 (7×10^{-30})**	−0.11 (0.048)	−0.012 (0.255)	0.019 (0.033)
Digit Span Backward	**0.37 (1×10^{-11})**	**−0.02 (2×10^{-19})**	−0.07 (0.208)	−0.003 (0.774)	0.008 (0.209)
Letter–Number	**0.42 (3×10^{-14})**	**−0.03 (7×10^{-48})**	0.07 (0.213)	−0.005 (0.565)	**0.040 (2×10^{-4})**
PCET Correct	**0.33 (6×10^{-12})**	**−0.03 (4×10^{-40})**	0.02 (0.789)	−0.003 (0.754)	0.001 (0.457)
Spatial Delayed Response	**0.23 (8×10^{-6})**	**−0.01 (7×10^{-7})**	−0.07 (0.216)	−0.029 (0.192)	0.000 (0.500)
Trails B	**0.49 (8×10^{-20})**	**0.03 (3×10^{-43})**	−0.17 (0.004)	−0.011 (0.304)	0.009 (0.162)
CVLT Learning	**0.36 (7×10^{-11})**	**−0.02 (2×10^{-23})**	**0.50 (1×10^{-17})**	−0.017 (0.137)	0.023 (0.054)
CVLT Delay	**0.32 (2×10^{-10})**	**−0.02 (2×10^{-16})**	**0.46 (2×10^{-15})**	−0.016 (0.045)	**0.055 (3×10^{-4})**
CVLT Recognition	**0.24 (2×10^{-5})**	**−0.01 (4×10^{-11})**	**0.38 (5×10^{-11})**	−0.023 (0.297)	0.001 (0.470)
Facial Memory	**0.36 (6×10^{-11})**	**−0.01 (2×10^{-7})**	**0.30 (7×10^{-7})**	**−0.047 (0.001)**	0.000 (0.500)
Facial Memory Delay	**0.44 (2×10^{-12})**	**−0.01 (7×10^{-10})**	**0.27 (9×10^{-6})**	−0.022 (0.027)	0.028 (0.012)
Digit–Symbol Memory	**0.38 (4×10^{-11})**	**−0.03 (1×10^{-44})**	0.07 (0.179)	−0.013 (0.229)	0.000 (0.500)
Penn Emotion	**0.25 (2×10^{-6})**	**−0.03 (2×10^{-39})**	0.13 (0.022)	−0.007 (0.550)	0.057 (0.008)
Matrix Reasoning	**0.55 (2×10^{-23})**	**−0.04 (5×10^{-71})**	0.04 (0.451)	0.001 (0.909)	0.003 (0.364)
Vocabulary	**0.77 (8×10^{-43})**	**−0.01 (9×10^{-11})**	−0.08 (0.166)	0.014 (0.034)	**0.013 (0.001)**
WASI IQ	**0.77 (1×10^{-44})**	**−0.01 (7×10^{-12})**	−0.05 (0.399)	0.012 (0.016)	0.009 (0.020)
Global FA	**0.49 (7×10^{-10})**	**−0.04 (1×10^{-56})**	−0.13 (0.035)	0.008 (0.457)	0.012 (0.174)
Corpus callosum body	**0.45 (5×10^{-10})**	**−0.03 (2×10^{-49})**	0.03 (0.651)	0.002 (0.892)	0.010 (0.239)
Corpus callosum genu	**0.59 (2×10^{-12})**	**−0.04 (1×10^{-58})**	−0.09 (0.145)	0.001 (0.879)	0.023 (0.043)
Corpus callosum splenium	**0.55 (2×10^{-12})**	**−0.03 (6×10^{-38})**	−0.14 (0.032)	0.011 (0.266)	0.015 (0.140)
Anterior limb internal capsule	**0.47 (1×10^{-8})**	**−0.03 (5×10^{-30})**	**−0.20 (0.002)**	0.010 (0.512)	0.011 (0.211)
Posterior limb internal capsule	**0.46 (1×10^{-7})**	**−0.02 (5×10^{-22})**	−0.02 (0.821)	0.024 (0.307)	0.000 (0.500)
Retrolenticular internal capsule	**0.27 (6×10^{-4})**	**−0.02 (1×10^{-22})**	**−0.24 (3×10^{-4})**	−0.019 (0.497)	0.042 (0.164)
Anterior corona radiata	**0.48 (8×10^{-10})**	**−0.04 (3×10^{-57})**	−0.05 (0.367)	0.000 (0.983)	0.031 (0.014)
Superior corona radiata	**0.57 (4×10^{-12})**	**−0.04 (2×10^{-52})**	0.14 (0.017)	−0.001 (0.938)	0.002 (0.419)
Posterior corona radiata	**0.44 (1×10^{-9})**	**−0.03 (9×10^{-40})**	0.02 (0.784)	0.003 (0.850)	0.008 (0.271)
Posterior thalamic	**0.44 (9×10^{-9})**	**−0.04 (2×10^{-57})**	0.06 (0.352)	0.005 (0.775)	0.012 (0.187)
Sagittal stratum	**0.37 (3×10^{-6})**	**−0.03 (8×10^{-43})**	−0.03 (0.676)	0.020 (0.217)	0.007 (0.323)
External capsule	**0.53 (3×10^{-10})**	**−0.03 (7×10^{-49})**	−0.13 (0.033)	−0.001 (0.933)	0.007 (0.294)
Cingulum gyrus	**0.44 (4×10^{-8})**	**−0.03 (1×10^{-37})**	**−0.27 (2×10^{-5})**	0.016 (0.506)	0.012 (0.146)
Cingulum hippo	**0.31 (1×10^{-4})**	**−0.01 (0.016)**	**−0.44 (6×10^{-10})**	0.002 (0.873)	0.025 (0.097)
Superior longitudinal fasciculus	**0.59 (6×10^{-13})**	**−0.03 (2×10^{-43})**	−0.06 (0.339)	0.007 (0.542)	0.008 (0.184)
Superior frontooccipital fasciculus	**0.43 (2×10^{-8})**	**−0.03 (7×10^{-33})**	0.03 (0.640)	−0.009 (0.623)	0.000 (0.500)

Bolded estimates significant after correction for multiple testing (FDR = 0.05). See *Materials and Methods* and *SI Materials and Methods* for information on parameter estimates and related *P* values. IP-CPT, Identical Pairs Continues Performance Test; PCET, Penn Conditional Exclusion Test; CVLT, California Verbal Learning Test; WASI, Wechsler Abbreviated Scale of Intelligence.

Heritability. Heritability estimates for the neurocognitive and white-matter measures are presented in Table 1 and Fig. 2; all were significant, after controlling for multiple testing.

Genetic and Environmental Correlations Between Neurocognition and White-Matter Integrity. Given that neurocognitive and FA measures are strongly influenced by aging and phenotypically correlated and heritable, bivariate correlations were performed to determine if shared genetic or environmental factors influence these traits. Focusing on traits with significant phenotypic correlations, six environmental correlations were significant after controlling for multiple testing (Table S1), including performance on Trails A and global FA ($\rho_e = -0.25$, $P = 0.001$), the splenium of the corpus callosum ($\rho_e = -0.24$, $P = 0.004$), the retrolenticular part of internal capsule ($\rho_e = -0.13$, $P = 0.004$), the posterior thalamic radiation ($\rho_e = -0.18$, $P = 0.002$), the sagittal stratum ($\rho_e = -0.25$, $P = 2 \times 10^{-4}$), and the external capsule ($\rho_e = -0.30$, $P = 0.001$). These correlations indicated that common environmental factors were associated with worsening cognitive performance and reduced white-matter integrity.

In contrast to environmental correlations, no genetic correlation reached significance, suggesting that different genetic factors influence neurocognition and white-matter integrity. Among neurocognitive traits phenotypically correlated with FA, Matrix Reasoning had a trend-level genetic correlation with the anterior limb of the internal capsule ($\rho_g = 0.24$, $P = 0.06$). Similarly, Penn Facial Memory was weakly genetically associated with the splenium of the corpus callosum ($\rho_g = 0.11$, $P = 0.09$). When examining all neurocognitive and white-matter parings, no genetic correlation was significant after controlling for multiple testing (Fig. 3), suggesting that neurocognition and FA-based white-matter incidences do not share genetic influences.

G × A Interaction. Eight of the neurocognitive traits exhibited significant G × A interactions (Table 1). Three neurocognitive measures had significant genetic variance changes with advancing age (Digit–Symbol Substitution, Semantic Fluency, and Penn Facial Memory), suggesting differential influences of the same genetic factors across the lifespan. Heritability estimates for all of these neurocognitive measures were predicted to decrease

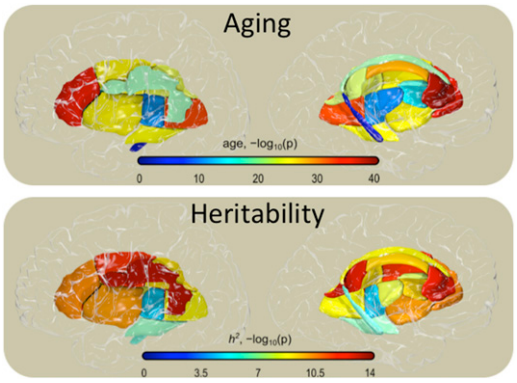

Fig. 2. The influence of aging and additive genetics on measures of tract-based white-matter integrity is presented. Though the *Upper* depicts linear effects of aging on tract-based FA measures, the *Lower* represents the heritability of each tract. All tracts were significantly heritable and strongly effected by aging. Fig. S1 provides reference labels for tracts.

over the age range assessed in this study (Fig. 4*A*). Five neurocognitive had significant changes in their genetic correlation (ρ_g) with age, suggesting that different genes influenced these traits from young adulthood to old age; these included tests of working and declarative memory (Letter–Number Span and CVLT Delay), processing speed (Trails A and Verbal Fluency), and Wechsler Abbreviated Scale of Intelligence (WASI) Vocabulary, indicating that heritable changes in neurocognitive functioning was not restricted to a single cognitive domain. Genetic correlation decreased as function of advancing age for each of these neurocognitive traits (Fig. 4*B*).

In contrast to neurocognition, no white-matter tract showed a significant G × A interaction (Table 1). The interaction term for each neurocognitive trait and age (γ for σ_g^2 variation with age and λ for ρ_g variation with age; *SI Materials and Methods*) and each white-matter trait and age are portrayed in Fig. 4*C*. Parameter estimates significantly differed between these classes of phenotypes for interactions modeling changes in σ_g^2 (neurocognitive average −0.013 vs. white-matter average 0.005, P = 0.0001) and changes in ρ_g (0.019 vs. 0.013, P = 0.24) with age.

Effects of Education. Given that older individuals had significantly fewer years of education (mean = 9.31 y for individuals older than 70) relative to younger individuals (mean = 11.61 y for individuals younger than 20), it is possible that differences in education exacerbate age-related cognitive or white-matter decline. However, because educational attainment was significantly heritable in this sample ($h^2 = 0.64$, $P = 1.5 \times 10^{-43}$), and because genetic variants associated with education also appear to be associated with cognitive functioning (28), it is unclear if controlling for educational attainment biases results by removing genetic variance associated with neurocognitive ability. Nonetheless, even when controlling for education attainment, significant G × A interactions are observed for measures of processing speed, working memory, and declarative memory (Table S2).

Discussion

In a large cohort of randomly selected related individuals, we documented substantial effects of aging on neurocognitive functioning and white-matter integrity. Both classes of traits are under considerable genetic control. However, results indicate that distinct genetic factors influence neurocognition and factional anisotropy, suggesting that these measures may reflect disparate genetic pathways of biological aging. Furthermore, G × A interaction analyses, which directly tested changes in genetic influence with aging, identified that the heritability of processing speed, attention, and memory measures changed with advancing age. These results imply that fluctuations in genetic influence with advancing age trigger at least a portion of the neurocognitive decline seen in normal aging. Our analyses suggest that for some traits, G × A interactions are due to changes in the action of specific genes, whereas for other measures, G × A interactions are associated with differences in the exact genes that influence the trait. Despite substantial power to detect effects, we found no evidence for significant G × A interaction for DTI traits, suggesting that age-related changes in white-matter integrity are less influenced by genetic factors. There is considerable theoretical debate whether the physical and cognitive changes associated with aging are intrinsically "programmed" or are incidental to the cumulative exposure to detrimental environmental elements (29, 30). Though this debate has fundamental ramifications for our understanding of the biology of aging, genes likely regulate both one's developmental program (31–33) and robustness to environmental exposures (34, 35). In the case of neurocognitive functioning, our data suggest that either model is viable. In contrast, changes in white-matter integrity appear more consistent with the model positing that robustness to environmental exposures drives FA declines with age.

Our results do not imply that white-matter integrity is not influenced by genetic factors. Indeed, we found significant heritability estimates for all tracts. Rather, our findings suggest that the changes in FA measures from young adulthood to old age are unlikely to be under substantial genetic control. Our results in the adult component of the human life course contrast with evidence from developmental biology that specific genes influence neuronal migration and the formation of white-matter tracts (31), and that DTI measures are strongly influenced by genetic factors during early childhood into early adolescence (36), suggesting that once the brain is mature, variation in the coherence of white-matter tracts is not directly controlled by genetic factors.

We observed a substantial decrease in neurocognitive and DTI measures from young adulthood to old age, replicating several prior reports (6, 37). Also, consistent with the literature, we found evidence for modest phenotypic correlations between neurocognitive and white-matter integrity, particularly for tests of speed of processing (27, 38, 39), working and declarative memory (12, 13), and IQ (14, 25). However, our findings extend this work by

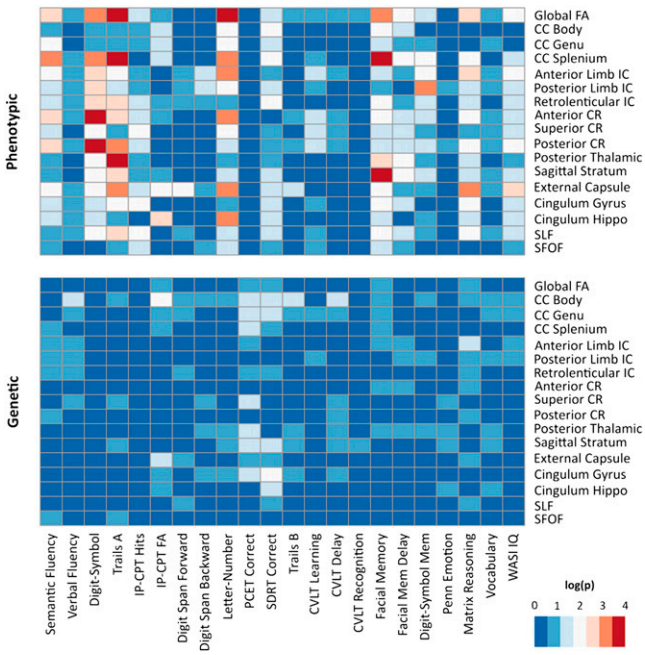

Fig. 3. A heat map reflecting –log P values for phenotypic and genetic correlations between neurocognitive and tract-based white-matter integrity measures from 809 individuals (see Table S1 for more detail). Though a number of significant phenotypic correlations were estimated, no genetic correlation was significant.

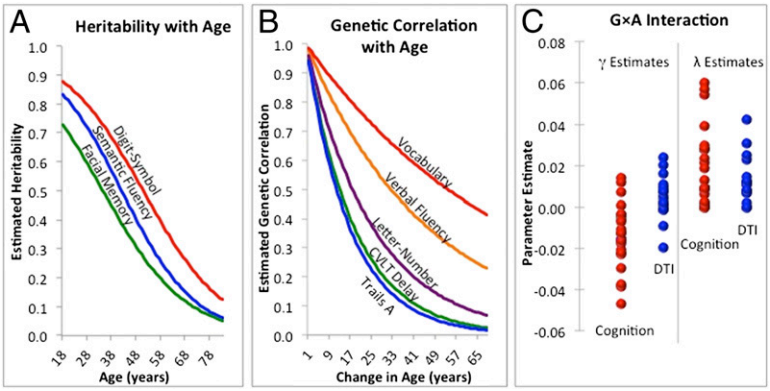

Fig. 4. Predicted changes in heritability (*A*) or genetic correlation (*B*) with age and the formal interaction terms (*C*) for neurocognitive and white-matter integrity traits generated via a gene-by-environment interaction analysis conducted with cross-sectional data in extended pedigrees where aging was treated as an environmental factor (e.g., G × A interaction analysis). (*A*) Additive genetic heritabilities as a function of age for traits that showed significant changes in genetic variance (σ_g^2) with age. (*B*) Significant changes in the genetic correlation (ρ_g) as functions of advancing age. (*C*) Scatter plot of all of the standardized G × A interaction terms for σ_g^2 (parameter estimate γ) or ρ_g (parameter estimate λ) for the neurocognitive and white-matter traits separately. The distribution of these interaction terms differed significantly between these classes of traits (γ neurocognitive −0.013 vs. γ white matter 0.005, $P = 0.0001$).

suggesting that these correlations are primarily of an environmental, rather than genetic, nature. This observation is consistent with findings that white-matter microstructure can change when individuals learn new skills (40, 41), even in old age (42), suggesting that environmental changes (e.g., learning to juggle) can influence FA levels. One implication from our analysis is that different genetic factors influence neurocognitive performance and white-matter FA in adulthood. Though it is quite possible that the same biological pathways influence both brain structure and cognitive function, our results suggest that different genes, potentially within the same putative network, influence these traits. Consequently, it appears that neurocognitive and white-matter integrity measures are influenced by unique genetic factors, implying that different genes may be associated with age-related neurocognitive decline and reduced white-matter coherence.

Improving our understanding of the biological mechanisms responsible for brain aging is clearly a pressing public health concern. Here, we document that G × A interaction analysis in extended pedigrees is well suited for discovering genes influencing brain aging. Identifying one or more genes that controls even a portion of the variance associated with brain aging should provide a causal anchor to focus subsequent biological inferences, informing this debate and providing clues into the aging process within other organ systems. Clear demonstration of G × A interactions in readily measurable and reliable brain aging phenotypes is an important first step in this scientific process.

Materials and Methods

Participants. English-speaking Mexican–American individuals from large extended pedigrees [81 pedigrees, average family size 14.95 (1–130) people] who participate in the Genetics of Brain Structure and Function study were included in the analysis ($n = 1{,}129$). Individuals in this cohort were randomly selected from the community, with the constraints that they are of Mexican–American ancestry, are part of a large family, and live within the San Antonio region (see ref. 50 for recruitment details). No other inclusion or exclusion criteria were imposed. However, individuals were excluded from the neurocognitive evaluation for history of neurological illnesses, stroke, or other major neurological event. Individuals were excluded from the neuroimaging evaluation for these criteria and for MRI contraindications. Reported pedigree relationships were empirically verified with autosomal markers. All participants provided written informed consent on forms approved by the Institutional Review Board at the University of Texas Health Science Center San Antonio (UTHSCSA)/Texas Biomedical Research Institute and the Human Investigation Committee (HIC) at Yale University.

Neurocognitive Assessment. Each participant completed a 90-min neuropsychological test battery consisting of standard and computerized measures (23, 44). Twenty-two neurocognitive variables were derived from 16 separate neuropsychological tests, including measures of attention, executive processing, working memory, declarative memory, language processing, intelligence, and emotional processing (Table S3).

Neuroimaging Assessment. Scanning was conducted at the Research Imaging Institute, UTHSCSA, using a Siemens Trio 3T system (Siemens) with a multichannel head coil. DTI data acquisition used a single-shot single spin-echo, echo-planar imaging sequence with a spatial resolution of 1.7 × 1.7 × 3.0 mm (repetition time/echo time = 8,000/87 ms, field of view = 200 mm, 55 nonparallel gradient directions b = 700 s/mm^2 and three non–diffusion-weighted images b = 0). DTI scans were preprocessed using standard FSL pipelines (http://fsl.fmrib.ox.ac.uk/fsl/fslwiki/FDT), and the resulting FA images were processed with tract-based spatial statistics (TBSS) (45). All FA images were nonlinearly registered to standard space, averaged, and skeletonized to create a study-specific TBSS template (binarized at FA > 0.2). Next, the maximum nearby FA voxel was projected onto the skeleton, resulting in one skeleton image per subject, reflecting FA values of the centers of the white-matter structure for that individual. For each subject, mean FA values were calculated for 16 tracts (bilateral) as defined by the Johns Hopkins White Matter Atlas (46) (Fig. S1). In addition, a global FA measure, reflecting the average FA throughout the white-matter skeleton, was derived.

Quantitative Genetic Analyses. All genetic analyses were conducted with SOLAR, which employs maximum-likelihood variance decomposition methods to determine the relative importance of familial and environmental influences on a measure, by modeling the covariance among family members as a function of genetic proximity (kinship). Neurocognitive and neuroimaging variables underwent a direct normalization with an inverse Gaussian transformation. Tests of variance component parameters were performed using standard likelihood ratio tests in which the *ln* likelihood of the null model (focal variance component constrained to zero) is compared with that of the alternative model (focal variance component is explicitly estimated from the data). To control for multiple testing, the false discovery rate (FDR) (47) was set at 5% for neurocognitive and DTI traits independently. Heritability, bivariate, and G × A interaction analyses included age and sex as demographic covariates.

Heritability (h^2) represents the portion of the phenotypic variance (σ^2_p) accounted for by additive genetic variance ($h^2 = \sigma^2_g/\sigma^2_p$). Indices with stronger phenotypic covariance between genetically more similar individuals than between genetically less similar individuals have higher heritability; within SOLAR, this is assessed by contrasting the observed covariance matrices for a measure with the covariance matrix predicted by kinship.

Bivariate polygenic analyses were performed to estimate the phenotypic (ρ_p), genetic (ρ_g), and environmental (ρ_e) correlations between neurocognitive and white-matter measures. The significance of these correlations was tested by comparing the *ln* likelihood for two restricted models (with either ρ_g or ρ_e constrained to equal 0.0) against the *ln* likelihood for the model in which these parameters were estimated. A significant genetic correlation is evidence for pleiotropy, that a gene or set of genes influences both phenotypes (48). In contrast, a significant environmental correlation is evidence that common nongenetic factors influence both traits.

Difference in genetic variance in response to environmental change (including the physiological environment, age) is evidence of a G × E interaction. Although aging is a continuous process, it is conceptually useful to explain the relationship between G × E interaction and the heritable response to environmental change in terms of two discrete environments. The additive genetic variance in response ($\sigma^2_{g\Delta}$) is a function of the additive genetic variance expressed in the two environments and the additive genetic correlation between the trait's expression in the two environments:

$$\sigma^2_{g\Delta} = \sigma^2_{g1} + \sigma^2_{g2} - 2\rho_g\sigma_{g1}\sigma_{g2} = (\sigma_{g1} - \sigma_{g2})^2 + 2\sigma_{g1}\sigma_{g2}(1 - \rho_g).$$

The absence of G × E interaction implies that there is no genetic variance for the response to the environment (i.e., $\sigma^2_{g\Delta} = 0$). This equation, initially

derived by Robertson (49), shows that there is no G × E interaction when $\sigma^2_{g1} = \sigma^2_{g2}$ and $\rho_g = 1$. The first condition requires that the genetic variance be constant across environments. Observed heteroscedasticity of genetic variances across environments can arise simply because of scaling. For example, if $g_2 = cg_1$, where c is a constant, σ^2_{g2} will be equal to $c^2\sigma^2_{g1}$ and $(\sigma_{g1} - \sigma_{g1})^2$ will equal $(1-c)^2\sigma^2_{g1}$. For the second condition ($\rho_g = 1$) to hold, the same genes must influence the phenotype in both environments and have similar effects in each. The second condition is the requirement of complete pleiotropy. In the absence of complete pleiotropy ($\rho_g < 1$), the genotypes may exhibit different ranks in different environments: one genotype may express the highest quantitative trait mean in one environment but a different genotype may have the highest mean in a second environment.

For continuous environments such as aging, these relationships are replaced with parametric continuous functions of the environment (21). Specifically, the discrete two-environment model is extended to reflect pairwise differences in environment between subjects, thereby sampling the full range of subject ages in the cross-sectional sample (21, 50, 51). The hypothesis in the extended model is that the phenotypic covariance between individuals is a function of interaction between their similarity in age and their genetic similarity. This relationship may be due to age-related changes in genetic variance, $\rho_g < 1$ between measurements of the trait at different ages, or both (22). See *SI Materials and Methods* for more detail.

We found evidence of G × A interaction for some neurocognitive traits but for no white-matter trait. Because fewer individuals provided white-matter than neurocognitive data, we performed formal analytical power calculations using our exact data structure to assess our potential to detect true effects in all traits (had these been present) of the same magnitude as those we observed (51). For the test of $\sigma^2_{g1} = \sigma^2_{g2}$, all traits had >97% power to detect such effects. The power was less, but still substantial (range 63–89%), for the test of $\rho_g = 1$. Thus, our power to detect G × A interaction is considerable. Therefore, our inference that white-matter decline is not influenced by moderate to strong G × A interaction and hence is not strongly heritable is likely to be true in this population.

ACKNOWLEDGMENTS. We thank participants of the San Antonio Family Study and our research staffs. Financial support for this study was provided by National Institute of Mental Health Grants MH0708143 (to D.C.G.), MH078111 (to J.B.), and MH083824 (to D.C.G. and J.B.). Theoretical development of the G × A model and its implementation in SOLAR is supported by National Institute of Mental Health Grants MH59490 (to J.B.) and EB015611 (to P.K.). This investigation was conducted, in part, in facilities constructed with support from Research Facilities Improvement Program Grants C06 RR13556 and C06 RR017515 from the National Center for Research Resources, National Institutes of Health. The supercomputing facilities used for this work at the AT&T Genomics Computing Center were supported, in part, by a gift from the AT&T Foundation and by National Center for Research Resources Grant S10 RR029392.

1. US Census Bureau Population Division and Housing and Household Economic Statistics Division (2008) *National Population Projections* (US Census Bureau, Suitland, MD).
2. Rowe JW, Kahn RL (1987) Human aging: Usual and successful. *Science* 237(4811):143–149.
3. Bishop NA, Lu T, Yankner BA (2010) Neural mechanisms of ageing and cognitive decline. *Nature* 464(7288):529–535.
4. Glorioso C, Sibille E (2011) Between destiny and disease: Genetics and molecular pathways of human central nervous system aging. *Prog Neurobiol* 93(2):165–181.
5. Glatt SJ, Chayavichitsilp P, Depp C, Schork NJ, Jeste DV (2007) Successful aging: From phenotype to genotype. *Biol Psychiatry* 62(4):282–293.
6. Buckner RL (2004) Memory and executive function in aging and AD: Multiple factors that cause decline and reserve factors that compensate. *Neuron* 44(1):195–208.
7. Hedden T, Gabrieli JD (2004) Insights into the ageing mind: A view from cognitive neuroscience. *Nat Rev Neurosci* 5(2):87–96.
8. Hultsch DF, Hertzog C, Small BJ, Dixon RA (1999) Use it or lose it: Engaged lifestyle as a buffer of cognitive decline in aging? *Psychol Aging* 14(2):245–263.
9. Pfefferbaum A, Adalsteinsson E, Sullivan EV (2005) Frontal circuitry degradation marks healthy adult aging: Evidence from diffusion tensor imaging. *Neuroimage* 26(3):891–899.
10. Kochunov P, et al. (2010) Genetics of microstructure of cerebral white matter using diffusion tensor imaging. *Neuroimage* 53(3):1109–1116.
11. Giorgio A, et al. (2010) Age-related changes in grey and white matter structure throughout adulthood. *Neuroimage* 51(3):943–951.
12. Kennedy KM, Raz N (2009) Aging white matter and cognition: Differential effects of regional variations in diffusion properties on memory, executive functions, and speed. *Neuropsychologia* 47(3):916–927.
13. Deary IJ, et al. (2006) White matter integrity and cognition in childhood and old age. *Neurology* 66(4):505–512.
14. Borghesani PR, et al. (2013) The association between higher order abilities, processing speed, and age are variably mediated by white matter integrity during typical aging. *Neuropsychologia* 51(8):1435–1444.
15. Kantarci K, et al. (2011) Diffusion tensor imaging and cognitive function in older adults with no dementia. *Neurology* 77(1):26–34.
16. Charlton RA, et al. (2006) White matter damage on diffusion tensor imaging correlates with age-related cognitive decline. *Neurology* 66(2):217–222.
17. Bendlin BB, et al. (2010) White matter in aging and cognition: A cross-sectional study of microstructure in adults aged eighteen to eighty-three. *Dev Neuropsychol* 35(3):257–277.
18. Penke L, et al. (2010) A general factor of brain white matter integrity predicts information processing speed in healthy older people. *J Neurosci* 30(22):7569–7574.
19. Brans RG, et al. (2010) Brain plasticity and intellectual ability are influenced by shared genes. *J Neurosci* 30(16):5519–5524.
20. Karlsgodt KH, et al. (2010) A multimodal assessment of the genetic control over working memory. *J Neurosci* 30(24):8197–8202.
21. Blangero J (1993) Statistical genetic approaches to human adaptability. *Hum Biol* 65(6):941–966.
22. Kent JW, Jr., et al. (2012) Genotype × age interaction in human transcriptional ageing. *Mech Ageing Dev* 133(9-10):581–590.
23. Glahn DC, et al. (2010) Neurocognitive endophenotypes for bipolar disorder identified in multiplex multigenerational families. *Arch Gen Psychiatry* 67(2):168–177.
24. Salthouse TA (1992) What do adult age differences in the Digit Symbol Substitution Test reflect? *J Gerontol* 47(3):121–128.
25. Charlton RA, et al. (2008) A structural equation modeling investigation of age-related variance in executive function and DTI measured white matter damage. *Neurobiol Aging* 29(10):1547–1555.
26. Bucur B, et al. (2008) Age-related slowing of memory retrieval: Contributions of perceptual speed and cerebral white matter integrity. *Neurobiol Aging* 29(7):1070–1079.
27. Turken A, et al. (2008) Cognitive processing speed and the structure of white matter pathways: Convergent evidence from normal variation and lesion studies. *Neuroimage* 42(2):1032–1044.
28. Rietveld CA, et al.; LifeLines Cohort Study (2013) GWAS of 126,559 individuals identifies genetic variants associated with educational attainment. *Science* 340(6139):1467–1471.
29. Charlesworth B (2000) Fisher, Medawar, Hamilton and the evolution of aging. *Genetics* 156(3):927–931.
30. Holliday R (2006) Aging is no longer an unsolved problem in biology. *Ann N Y Acad Sci* 1067:1–9.
31. Rakic P (1988) Specification of cerebral cortical areas. *Science* 241(4862):170–176.
32. Williams LM, Rudensky AY (2007) Maintenance of the Foxp3-dependent developmental program in mature regulatory T cells requires continued expression of Foxp3. *Nat Immunol* 8(3):277–284.
33. Henderson ST, Johnson TE (2001) Daf-16 integrates developmental and environmental inputs to mediate aging in the nematode *Caenorhabditis elegans*. *Curr Biol* 11(24):1975–1980.
34. Christensen BC, et al. (2009) Aging and environmental exposures alter tissue-specific DNA methylation dependent upon CpG island context. *PLoS Genet* 5(8):e1000602.
35. Hunter DJ (2005) Gene–environment interactions in human diseases. *Nat Rev Genet* 6(4):287–298.
36. Brouwer RM, et al. (2012) White matter development in early puberty: A longitudinal volumetric and diffusion tensor imaging twin study. *PLoS ONE* 7(4):e32316.
37. Kochunov P, et al. (2012) Fractional anisotropy of water diffusion in cerebral white matter across the lifespan. *Neurobiol Aging* 33(1):9–20.
38. Tuch DS, et al. (2005) Choice reaction time performance correlates with diffusion anisotropy in white matter pathways supporting visuospatial attention. *Proc Natl Acad Sci USA* 102(34):12212–12217.
39. Jacobs HI, et al. (2013) Association between white matter microstructure, executive functions, and processing speed in older adults: The impact of vascular health. *Hum Brain Mapp* 34(1):77–95.
40. Scholz J, Klein MC, Behrens TE, Johansen-Berg H (2009) Training induces changes in white-matter architecture. *Nat Neurosci* 12(11):1370–1371.
41. Bengtsson SL, et al. (2005) Extensive piano practicing has regionally specific effects on white matter development. *Nat Neurosci* 8(9):1148–1150.
42. Lövdén M, et al. (2010) Experience-dependent plasticity of white-matter microstructure extends into old age. *Neuropsychologia* 48(13):3878–3883.
43. Olvera RL, et al. (2011) Common genetic influences on depression, alcohol, and substance use disorders in Mexican-American families. *Am J Med Genet B Neuropsychiatr Genet* 156B(5):561–568.
44. Glahn DC, et al. (2007) Adjudicating neurocognitive endophenotypes for schizophrenia. *Am J Med Genet B Neuropsychiatr Genet* 144B(2):242–249.
45. Smith SM, et al. (2006) Tract-based spatial statistics: Voxelwise analysis of multi-subject diffusion data. *Neuroimage* 31(4):1487–1505.
46. Benjamini Y, Hochberg Y (1995) Controlling the false discovery rate: A practical and powerful approach to multiple testing. *J R Stat Soc B* 57:289–300.
47. Almasy L, Dyer TD, Blangero J (1997) Bivariate quantitative trait linkage analysis: Pleiotropy versus co-incident linkages. *Genet Epidemiol* 14(6):953–958.
48. Robertson A (1959) The sampling variance of the genetic correlation coefficient. *Biometrics* 15:469–485.
49. Almasy L, Towne B, Peterson C, Blangero J (2001) Detecting genotype × age interaction. *Genet Epidemiol* 21(Suppl 1):S819–S824.
50. Diego VP, Almasy L, Dyer TD, Soler JM, Blangero J (2003) Strategy and model building in the fourth dimension: A null model for genotype × age interaction as a Gaussian stationary stochastic process. *BMC Genet* 4(Suppl 1):S34.
51. Diego VP (2005) Genotype (age interaction, and the insulin-like growth factor I axis in the San Antonio Family Heart Study: A study in human senescence. PhD thesis (State Univ of New York, Binghamton, NY).

Supporting Information

Glahn et al. 10.1073/pnas.1313735110

SI Materials and Methods

We conducted the cross-sectional genotype × age interaction analyses for this study using a modification of the standard variance components model implemented in SOLAR (1). Derivation of this model can be found in refs. 2–4. The Tcl script that implements the continuous-environment G × E analysis within SOLAR is available upon request from the authors. Briefly, the script performs the following sequence of steps:

1. The polygenic model for the trait of interest is reparameterized using the SOLAR polygsd command to replace the standardized variance components (heritability and standardized error variance) with the respective variances. Note that the trait value for an individual i can be decomposed as

$$y_i = \mu + \mathbf{x}_i\boldsymbol{\beta} + a_i + e_i, \qquad \textbf{[S1]}$$

where μ is the trait mean, $\mathbf{x}_i$ a vector of covariate measures, β is a vector of regression coefficients, a_i is the deviation from the mean due to additive genetic effects, and e_i is residual error. After regressing out the covariate effects, the covariance of the trait residuals for any two individuals i, j can be decomposed as

$$\mathrm{cov}_{i,j} = \phi_{i,j}\,\sigma^2_a + I_{i,j}\,\sigma^2_e, \qquad \textbf{[S2]}$$

where $\Phi_{i,j}$ is the expected proportion of alleles shared identical by descent across the autosomal genome; σ^2_a and σ^2_e are, respectively, the additive genetic and residual components of total phenotypic variance; and $I_{i,j}$ is an indicator variable that is 1 if i and j are the same individual and 0 otherwise (1).

2. The additive genetic variance in the covariance decomposition is restated as an exponential function of age as follows:

$$\sigma^2_a = \left[\exp(\alpha_a + \gamma_a\delta_i)\right]^{0.5} \times \left[\exp(\alpha_a + \gamma_a\delta_j)\right]^{0.5} \times \exp\left(-\lambda \times |\delta_i - \delta_j|\right), \qquad \textbf{[S3]}$$

where δ is each individual's deviation in age from the cohort mean; α_a and γ_a are, respectively, parameters that reflect the portions of additive genetic variance that are unresponsive and responsive to age; and λ is a parameter that reflects the genetic correlation between measures of the trait in i and j. (If the ages of measurement are identical, the genetic correlation = 1; this is also the null hypothesis for the test of correlation-type G × A interaction.) The error variance term in Eq. **S2** is similarly restated as

$$\sigma^2_e = \exp(\alpha_e + \gamma_e\delta_i). \qquad \textbf{[S4]}$$

Note that the indicator variable in Eq. **S2** limits estimation of this component to cases where i and j are the same person. There is no correlation term because, in the cross-sectional design, each individual is measured on the trait at a single time.

1. Almasy L, Blangero J (1998) Multipoint quantitative-trait linkage analysis in general pedigrees. *Am J Hum Genet* 62(5):1198–1211.
2. Blangero J (1993) Statistical genetic approaches to human adaptability. *Hum Biol* 65(6): 941–966.
3. Almasy L, Towne B, Peterson C, Blangero J (2001) Detecting genotype × age interaction. *Genet Epidemiol* 21(Suppl 1):S819–S824.
4. Diego VP, Almasy L, Dyer TD, Soler JM, Blangero J (2003) Strategy and model building in the fourth dimension: A null model for genotype × age interaction as a Gaussian stationary stochastic process. *BMC Genet* 4(Suppl 1):S34.

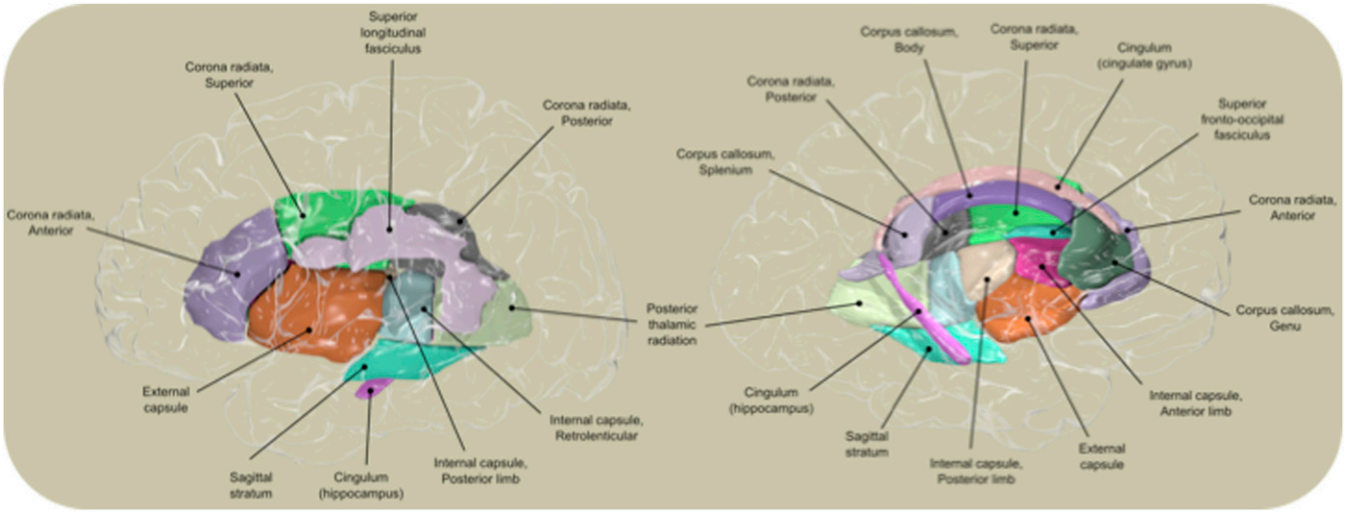

Fig. S1. Each white-matter tract is labeled for reference and reflects the average FA across hemispheres, as defined in the Johns Hopkins White Matter Atlas (1).

1. Mori S, et al. (2008) Stereotaxic white matter atlas based on diffusion tensor imaging in an ICBM template. *NeuroImage* 40:570–582.

Other Supporting Information Files

Table S1 (DOC)
Table S2 (DOC)
Table S3 (DOC)